Journal of Inorganic Biochemistry 195 (2019) 194–200

Contents lists available at ScienceDirect

Journal of Inorganic Biochemistry

journal homepage: www.elsevier.com/locate/jinorgbio

The crystal structure of the CopC protein from *Pseudomonas fluorescens* reveals amended classifications for the CopC protein family

Saumya R. Udagedara[a], Chathuri J.K. Wijekoon[b], Zhiguang Xiao[b], Anthony G. Wedd[b], Megan J. Maher[a,*]

[a] Department of Biochemistry and Genetics, La Trobe Institute for Molecular Science, La Trobe University, Melbourne 3083, Australia
[b] School of Chemistry and Bio21 Molecular Science and Biotechnology Institute, University of Melbourne, Parkville, Victoria 3010, Australia

ARTICLE INFO

Keywords:
CopC
Metallochaperone
Copper binding
X-ray crystallography

ABSTRACT

The bacterial CopC family of proteins are periplasmic copper binding proteins that act in copper detoxification. These proteins contain Cu(I) and/or Cu(II) binding sites, with the family that binds Cu(II) only the most prevalent, based on sequence analyses. Here we present three crystal structures of the CopC protein from *Pseudomonas fluorescens* (*Pf*-CopC) that include the wild type protein bound to Cu(II) and two variant proteins, where Cu(II) coordinating ligands were mutated, in Cu-free states. We show that the Cu(II) atom in *Pf*-CopC is coordinated by two His residues, an Asp residue and the N-terminus of the protein (therefore a 3N + O site). This coordination structure is consistent with all structurally characterized proteins from the CopC family to date. Structural and sequence analyses of the CopC family allow a relationship between protein sequence and the Cu (II) binding affinity of these proteins to be proposed.

1. Introduction

Copper is an essential cofactor in the catalytic sites of a wide range of enzymes that participate in processes such as respiration [1], antioxidant defence [2], iron homeostasis and the biogenesis of collagen and elastin [3]. However, it is toxic when in excess or dysregulated. The primary problem appears to be displacement of other essential metals from their native sites [4,5] and impairment of protein folding due to non-specific binding [6]. In addition, redox cycling of copper may lead to catalytic generation of reactive oxygen species (ROS) and other toxic products [7–10]. A delicate balance is required between intracellular copper excess and deficiency and specific homeostatic pathways have evolved to control copper metabolism in diverse forms of life [7,11,12].

Several copper regulatory systems have been characterized in Gram-negative bacteria, including the *cue*, *cus* and *cop/pco* gene clusters [7–9,13]. The chromosomally encoded tolerance operons *cue* and *cus* function in copper export and detoxification [13,14]. The *cue* system (Cu efflux) includes a trans-membrane P_{1B}-type ATPase (CopA) that facilitates Cu(I) efflux across the cell membrane to the periplasm. In Gram-negative bacteria such as *Escherichia coli*, a periplasmic multicopper oxidase CueO catalyzes the oxidation of Cu(I) to the less toxic Cu(II), while a cytoplasmic copper binding regulatory protein (CueR) completes this system that functions predominantly under aerobic conditions [15–18]. The *cus* system (Cu sensing) operates under anaerobic conditions [19]. It includes four proteins, CusABCF in *E. coli* [20], together with two regulatory proteins CusR and CusS [21]. CusABC is a tripartite complex that spans the entire periplasmic envelope and facilitates efflux of both Cu(I) and Ag(I) ions, driven by a proton gradient [22–25]. CusF is a periplasmic copper chaperone that delivers Cu(I) to the complex [26].

In addition to these genomic efflux and detoxification systems, some bacteria have acquired additional copper resistance mechanisms in order to survive in environments with elevated Cu levels. These systems originate from plasmid-borne genes and are termed the *cop/pco* systems (copper resistance, or plasmid-borne copper resistance) [8,27–30]. Even though these plasmid-borne resistance systems are present in bacteria, it is not yet clear how they impart cellular copper resistance. It has been suggested that the constituent proteins have individual functions in import and efflux of copper into and out of the cytoplasm and that they function in the sequestration of copper in the periplasm. Of these functions, the former activity has been relatively under-investigated due to the fact that there is no known function for copper in the bacterial cytoplasm [31]. Therefore, a definitive model for the individual functions of proteins in the *cop/pco* systems and their contributions to bacterial copper resistance remains elusive.

The *pco* cluster in *E. coli* comprises seven genes, *pcoABCDpcoRSpcoE*,

* Corresponding author.
E-mail address: M.Maher@latrobe.edu.au (M.J. Maher).

https://doi.org/10.1016/j.jinorgbio.2019.03.007
Received 21 December 2018; Received in revised form 26 February 2019; Accepted 7 March 2019
Available online 21 March 2019

which encode the proteins PcoABCDE and is regulated by the two-component system, PcoRS [32]. Three soluble proteins (PcoA, PcoC, PcoE) [33–36] are expressed and translocated to the periplasm, and two copper permeases (PcoB and PcoD) are present in the outer and inner membranes, respectively. The *cop* operons found in the copper resistant bacterium *Pseudomonas* (*P*) *syringae* carry six genes, *copABCDcopRS*, with equivalent functions and protein products as those of their *pco* counterparts, suggesting conserved mechanisms of copper resistance across these bacteria. The CopABCD proteins from the *cop* operon are homologous to the PcoABCD proteins from plasmid-borne *pco* cluster. Similar to the *pco* operon, the *cop* operon is also regulated by a two-component system CopRS [35,37,38].

Both the Cop and Pco protein families include two soluble proteins that contain methionine-rich sequences: CopA, CopC and PcoA, PcoC in *P. syringae* and *E. coli*, respectively. The former proteins, CopA and PcoA are multicopper oxidases with functions comparable to that of the CueO protein [29,34]. The latter proteins, *P. syringae* CopC (*Ps*-CopC) and *E. coli* PcoC (*Ec*-PcoC) are proposed to act as copper chaperones in the oxidizing environment of the periplasm. Previous studies on these CopC proteins determined that they feature separate Cu(I) and Cu(II) binding sites [34,37,39,40]. Their structures are similar in topology (Greek key β-barrel folds) and have been reported in copper-loaded and *apo* forms [37,39]. Copper coordination was not observed in the structure of *Ec*-PcoC [39] since the recombinant protein used for crystallization did not include an N-terminal His residue, which is required for Cu(II) coordination [39]. In *Ps*-CopC, the Cu(I) atom is coordinated by Met and His residues and the Cu(II) atom is coordinated in a square planar geometry by the side chains of two His residues, the amino terminus, and a water molecule, with an Asp residue in hydrogen bonding distance of the coordinated water [37].

Recent studies on the CopC proteins from *Pseudomonas fluorescens* SBW25 (*Pf*) [41], *Methylosinus trichosporium* OB3b (*Mst*) [42] and *Thioalkalivibrio paradoxus* ARh 1 (*Tp*) [43] have revealed a class of CopC proteins that lack the Cu(I) binding site and that bind Cu(II) only. In addition, the open reading frames for these proteins are located on chromosomal (rather than plasmid-borne) *cop* operons that encode two Cop proteins (CopCD), rather than the usual four proteins, CopABCD [42,43]. The Cu(II) binding site has been characterized structurally for the *Mst*-CopC and *Tp*-CopC proteins. The Cu(II) binding sites in these structures include two His and one Asp side chains as ligands, in addition to the amino terminus of the protein. The Cu(II) site in *Mst*-CopC shows a distorted square planar geometry with an axial water molecule [42] while *Tp*-CopC Cu(II) site has a square-planar geometry [43]. The sequences of both proteins lack the conserved residues necessary for Cu (I) binding.

A recent extensive structural and bioinformatics study proposed the division of the CopC protein family into categories according to the absence (0), presence in the canonical form (1) and presence in a higher-affinity form (2) of the Cu(I) and Cu(II) sites within these proteins. Each bacterial CopC class was given a designation consisting of "C" followed by two subscript digits, of which the first identifies the type of Cu(I) site and the second identifies the type of Cu(II) site. This resulted in the proposal of five categories of CopC protein: $C_{0\text{-}1}$, $C_{0\text{-}2}$, $C_{1\text{-}1}$, $C_{0\text{-}0}$, $C_{1\text{-}0}$ (listed in order of prevalence) [42]. This analysis indicated that the $C_{0\text{-}1}$ CopC proteins are the most abundant, despite the fact that the majority of the structural and functional investigations of these proteins had so far concentrated on CopC proteins from the $C_{1\text{-}1}$ category (specifically the *Ps*-CopC and *Ec*-PcoC proteins), which represent only 5.4% of the analyzed CopC sequences. According to this classification, the *Mst*-CopC and *Pf*-CopC proteins were assigned to class $C_{0\text{-}1}$ and $C_{0\text{-}2}$, respectively. The classification of the *Pf*-CopC protein was based on the apparent high affinity of the protein for Cu(II) and the proposal of a remarkably different, but structurally unconfirmed putative Cu(II) coordination site in that protein [41].

Specifically, the *Pf*-CopC protein was characterized to feature a Cu (II) binding site with sub-femtomolar affinity at pH 7.4 and was proposed, based on site-specific mutations, to include a novel Cu(II) site that differed distinctly from that of the class $C_{1\text{-}1}$ CopC proteins [41]. The His residue at position 1 (using residue numbering for the mature protein, without the signal sequence) was proposed to act as a bidentate ligand, with the coordination site completed with ligands from both the His3 and His85 side chains (that is, a 4N binding site) [41]. Upon mutation of the His1 residue to Phe, an ATCUN binding mode (as observed for proteins such as the serum albumins) [44] was detected that was proposed to include residue His3, the N-terminal amine, and two deprotonated peptide backbone amides as co-ligands.

To define the structure of the Cu(II) binding site for the *Pf*-CopC protein and therefore categorize it within the CopC protein family, we present here the crystal structures of the Cu(II)-*Pf*-CopC protein and its coordination site mutants.

2. Materials and methods

2.1. Protein expression, purification and crystallization

Residue numbering for the *Pf*-CopC protein throughout this manuscript, including the structural descriptions and the submitted Protein Data Bank (PDB) coordinates follows the PDB convention, numbered according to the GenBank entry (YP_002873498). That is, residue numbering includes the signal sequence. Therefore, throughout this manuscript the N-terminal residue is numbered His25 (His1 in [41]).

The wild-type *Pf*-CopC (^{WT}*Pf*-CopC), H109F (^{H109F}*Pf*-CopC, referred to as H85F in [41]) and H25FH109F (^{DM}*Pf*-CopC, referred to as H1FH85F in [41]) mutant proteins were cloned, overexpressed, purified and copper loaded as previously described [41].

Crystallization conditions for the three CopC proteins were screened by hanging drop vapor diffusion in 96-well plates (Greiner Bio-One) using a Crystal Gryphon liquid handling robot (Art Robbins Instruments) and commercially available screens (Index, SaltRX, Hampton Research, Laguna Hills, CA) at 293 K. Crystals of the ^{H109F}*Pf*-CopC and ^{DM}*Pf*-CopC proteins appeared after one week in conditions F5 and C12 of the SaltRX screen (2.4 M sodium malonate pH 7.0, 0.1 M Bis-Tris propane pH 7.0 and 2.5 M $(NH_4)_2SO_4$, 0.1 M Bis-Tris propane pH 7.0, respectively). Further refinement of the crystallization conditions led to ^{H109F}*Pf*-CopC crystals grown in 2.5 M $(NH_4)_2SO_4$, 0.1 M Bis-Tris propane pH 6.7 and ^{DM}*Pf*-CopC crystals in 2.7 M $(NH_4)_2SO_4$, 0.1 M Bis-Tris propane pH 7.0.

For data collection, crystals were cryoprotected by brief immersion in a modified reservoir solution supplemented with glycerol (3 M $(NH_4)_2SO_4$, 25% (v/v) glycerol, 0.1 M Bis-Tris propane, pH 7.0) and flash-cooled in liquid nitrogen. ^{WT}*Pf*-CopC crystals appeared in conditions F5 and F6 of the SaltRX screen (2.5 M $(NH_4)_2SO_4$, 0.1 M Bis-Tris propane pH 7.0 and 2.5 M $(NH_4)_2SO_4$, 0.1 M Tris pH 8.5, respectively) and optimization led to the growth of diffraction quality crystals in 2.5 M $(NH_4)_2SO_4$, 0.1 M Bis-Tris propane pH 6.7, 2 mM $YCl_3{\cdot}6H_2O$. Crystals were cryoprotected by brief immersion in 3 M sodium malonate pH 7.0 and flash-cooled in liquid nitrogen for data collection.

2.2. Data collection, structure solution and refinement

Diffraction data were collected on the MX2 beamline at the Australian Synchrotron, equipped with an ADSC Quantum 315r detector. Data were processed and scaled using HKL2000 [45]. The crystal structures of all three proteins were solved by molecular replacement using the program PHASER [46] from the CCP4 suite [47]. The structure of the ^{H109F}*Pf*-CopC protein was solved using a search model generated by the program CHAINSAW [48] from the structure of the CopC protein from *P. syringae* (PDB code: 2C9Q) [37]. For the ^{WT}*Pf*-CopC and ^{DM}*Pf*-CopC structures, the refined structure of the ^{H109F}*Pf*-CopC was used as the search model. The structures were refined using REFMAC5, with iterative cycles of model building in COOT [46,47,49]. The ^{WT}*Pf*-CopC model includes three Cu atoms per asymmetric unit

Table 1
Diffraction data and refinement statistics.[a]

	^{WT}*Pf*-CopC	^{H109F}*Pf*-CopC	^{DM}*Pf*-CopC
Data collection			
Space group	$C222_1$	$P2_12_12_1$	$P2_12_12_1$
Unit cell parameters (Å, °)	77.7, 111.3, 82.2	30.03, 35.6, 95.6	30.6, 34.7, 94.7
Resolution (Å)	50.0–2.00 (2.07–2.00)	50.0–1.00 (1.04–1.00)	50.0–1.50 (1.55–1.50)
No. of observations	312,106	839,681	246,003
No. of unique reflections	24,385	52,044	16,927
Completeness (%)	100.0 (100.0)	92.9 (89.6)	99.8 (99.3)
Redundancy	6.0 (6.1)	2.4 (2.2)	6.8 (6.7)
R_{pim} (%)	7.8 (66.0)	4.2 (40.6)	3.5 (42.2)
R_{merge} (%)	17.6 (148)	7.5 (51.3)	8.7 (100)
$CC_{1/2}$ (highest resolution shell)	0.529	0.803	0.772
Average $I/\sigma(I)$	9.7 (1.2)	12.2 (1.8)	20.7 (2.0)
Refinement			
Resolution	46.0–2.00 (2.05–2.00)	33.0–1.00 (1.02–1.00)	33.0–1.50 (1.54–1.50)
R (%)	22.8 (32.3)	14.8 (29.9)	18.2 (25.7)
R_{free} (%)	26.0 (41.5)	17.2 (30.4)	21.1 (30.9)
No. (%) of reflections in test set	1238 (5.1)	2611 (5.0)	837 (5.0)
No. of protein molecules per asu	3	1	1
No. of Cu atoms per asu	3	0	0
R.m.s.d. bond length (Å)	0.010	0.006	0.012
R.m.s.d. bond angle (°)	1.37	1.24	1.54
Average *B*-factors (Å^2)[b]			
Protein	40.01	10.33	17.75
Water	37.79	21.66	27.15
Copper	16.71	–	–
Ramachandran plot[c]			
Residues other than Gly & Pro in:			
Most favoured regions (%)	97.5	100	99
Additional allowed regions (%)	2.5	0	1
Disallowed regions (%)	0	0	0
ESU (Å)[d]	0.104	0.019	0.05
PDB code	6NFQ	6NFR	6NFS

[a] Values in parentheses are for the highest-resolution shell.
[b] Calculated by BAVERAGE in CCP4 Suite [47].
[c] Calculated using Molprobity [50].
[d] Estimated overall coordinate error based on maximum likelihood as output from REFMAC [49].

(asu), which were refined with individual occupancies of 1.0. Anisotropic *B*-factor refinement was applied to the ^{H109F}*Pf*-CopC structure. Model geometry was analyzed by MOLPROBITY [50] and structure figures were generated with PyMOL (PyMOL Molecular Graphics System, Schrodinger, LLC).

3. Results and discussion

3.1. Structures of the CopC from Pseudomonas fluorescens SBW 25

We successfully crystallized the $^{Cu(II)WT}$*Pf*-CopC and the mutant proteins ^{H109F}*Pf*-CopC and ^{DM}*Pf*-CopC and solved the structures by molecular replacement. The $^{Cu(II)WT}$*Pf*-CopC protein crystallized in space group $C222_1$ and the structure was refined to 2.0 Å resolution, with residuals R = 22.8 and R_{free} = 25.9% and three $^{Cu(II)WT}$*Pf*-CopC molecules per asu (Table 1, Fig. 2). In this structure, a yittrium (Y) atom from the crystallization medium (at occupancy 0.5) lies on a crystallographic two-fold axis and bridges one of the $^{Cu(II)WT}$*Pf*-CopC molecules with a symmetry related partner. The Y(III) ion is coordinated by the side chains of residue Glu68 from the $^{Cu(II)WT}$*Pf*-CopC and its symmetry related partner and two water molecules. The superposition of all combinations of the three molecules in the asu yields r.m.s.d. values between 0.29 and 0.43 Å for 98 common Cα positions. Given these consistent structures, all structure descriptions for $^{Cu(II)WT}$*Pf*-CopC are for molecule A as representing all molecules in the asu.

Both mutant proteins, ^{H109F}*Pf*-CopC and ^{DM}*Pf*-CopC crystallized in space group $P2_12_12_1$. The structures were refined to 1.0 and 2.21 Å resolution, respectively, with a single molecule in the asu. Refinements converged with residuals R = 14.8, R_{free} = 17.2% and R = 18.2, R_{free} = 21.1% for the ^{H109F}*Pf*-CopC and ^{DM}*Pf*-CopC structures, respectively. All three *Pf*-CopC structures show excellent geometry (Table 1). The overall structures all reveal a seven-stranded Greek key β-barrel fold (Fig. 2).

3.2. The Cu(II) binding site structure in ^{WT}Pf-CopC is consistent with other structurally characterized proteins from the CopC family

The $^{Cu(II)WT}$*Pf*-CopC structure includes a single Cu(II) ion per protein molecule, which is coordinated by residues His25, His109, Asp107 and the amino terminus in a distorted tetragonal geometry (Table 2, Fig. 3). Previously it was proposed that the Cu(II) binding site in this protein featured a 4N binding site with coordination ligands including the N-terminal amine and the side chains of residues His25, His27 and His109 (i.e., His1, His3 and His85 in [41]). This proposal was made based on the effects of the mutation of putative Cu(II) binding ligands on

```
Tp-CopC       HAHLRAADPPEAIVDAAGLREIRLVFSEPVVDRFSTFRAFRLSLPENGIRNLTQLNTLAS 60
Mst-CopC      HSFLVDASPSAKDHVAASPKLVKLRFGGGVEPAYSSISILDST------------G---- 44
Pf-CopC       HAHLKSATPAADS-TVAAPADLRLTFSEGVEATFTKVSLSKDG------------T---- 43
Ps-CopC       HPKLVSSTPAEGS-EGAAPAKIELHFSENLVTQFSGAKLVMTAMP-----GME-HS---- 49
Ec-PcoC       HPELKSSVPQADS-AVAAPEKIQLNFSENLTVKFSGAKLTMTGMK-----GMSSHS---- 50

Tp-CopC       ELGVDTEESAHHEVELESDL--SSQSAEVTLHSDEPLPAGAYAVVWRVLSVDGHTTTGFH 118
Mst-CopC      ------------KLVVEGA-KGQADKPRELTLDAPELAVGSYVVKFRVLSSDGHIVEGKY 91
Pf-CopC       ------------EVAIKGLETPDADKKTLVVTPAAPLAAGNYKVVWNAVSVDTHKSNGEY 91
Ps-CopC       ------------PMAVKAAVSGGGDPKTMVITPASPLTAGTYKVDWRAVSSDTHPITGSV 97
Ec-PcoC       ------------PMPVAAKVAPGADPKSMVIIPREPLPAGTYRVDWRAVSSDTHPITGNY 98

Tp-CopC       AFVHAGGTASSH    130
Mst-CopC      EFTVDPHENLY-    102
Pf-CopC       SFKVGQ------    97
Ps-CopC       TFKVK-------    102
Ec-PcoC       TFTVK-------    103
```

Fig. 1. Multiple sequence alignment of the CopC proteins. Ligands for the Cu(I) and Cu(II) binding sites are highlighted in pink and cyan, respectively.

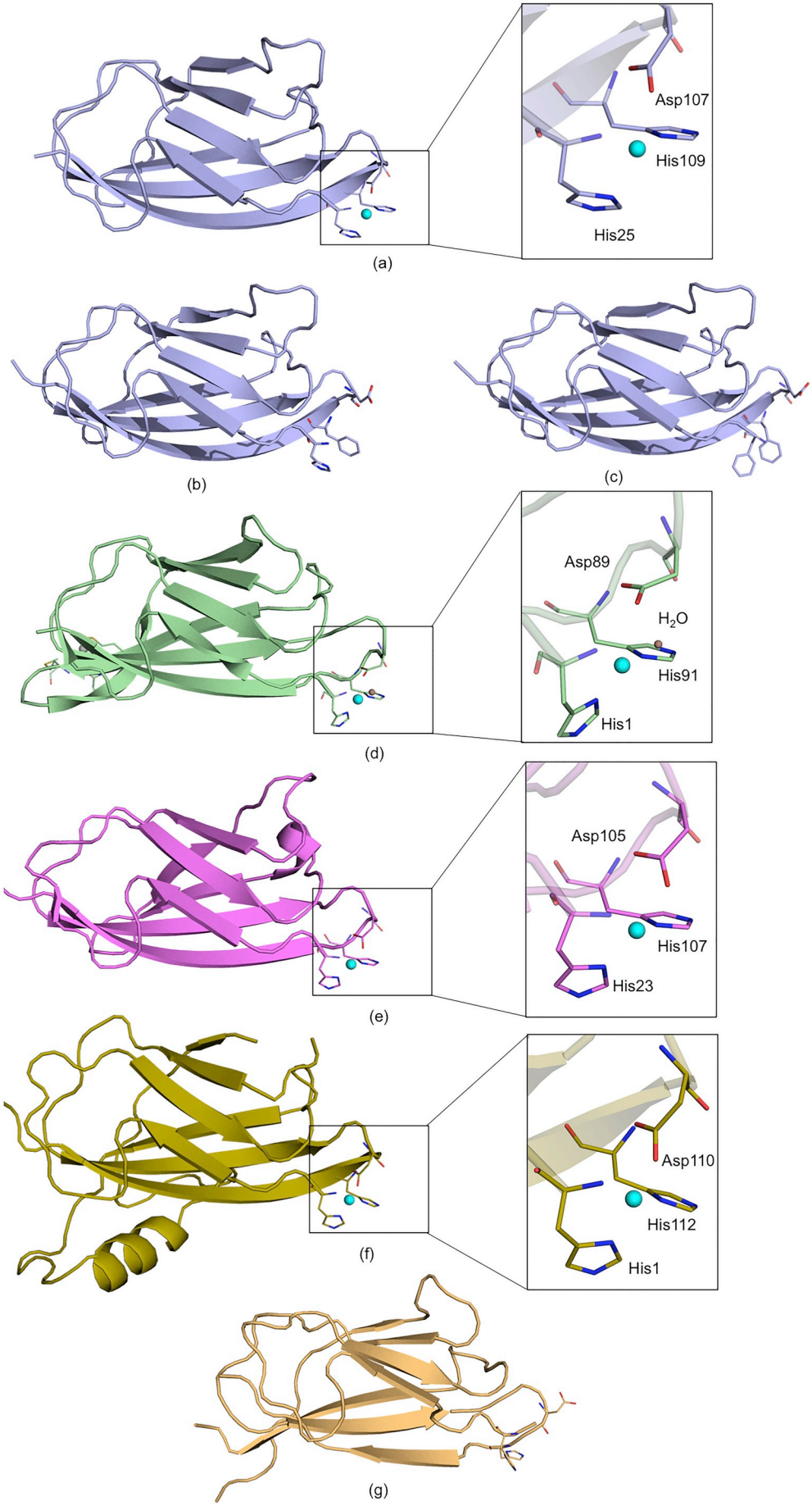

(caption on next page)

Fig. 2. Molecular structures of CopC proteins. In all panels, Cu(I) is represented as a gray sphere and Cu(II) in cyan. The coordinating ligands to the Cu(II) sites are labelled. (a) $^{Cu(II)WT}$*Pf*-CopC; (b) ^{H109F}*Pf*-CopC; (c) ^{DM}*Pf*-CopC; (d) $^{Cu(I)Cu(II)}$*Ps*-CopC (PDB 2C9Q) [37]; (e) $^{Cu(II)}$*Mst*-CopC (PDB 5ICU) [42]; (f) $^{Cu(II)}$*Tp*-CopC (PDB 5NLT) [43]; (g) *Ec*-PcoC (PDB 1LYQ) [39].

Table 2
Copper center geometry.

Bond distance to Cu(II) (Å)					
Pf-CopC	2.2 (2) (His25)	2.2 (2) (NH_2/His25)	2.1(2) (His109)	2.4 (2) (Asp107)	
Mst-CopC[a] [42]	2.06 (5) (His23)	2.03 (5) (NH_2/His23)	1.97 (5) (His107)	2.30 (5) (Asp105)	2.37 (5) (H_2O)
Ps-CopC [37]	2.18 (8) (His1)	1.96 (8) (NH_2/His1)	1.95 (8) (His91)	1.82 (8) (H_2O78)	
Tp-CopC[b] [43]	2.0 (4) (His1)	2.0 (4) (NH_2/His1)	2.0 (4) (His112)	1.9 (4) (Asp110)	
Bond angle (°)					
Pf-CopC	110.3 (His25-Cu-His109)	87.5 (His109-Cu-Asp107)	68.8 (Asp107-Cu-His25)	92.4 (NH_2/His25-Cu-His25)	

[a,b]The error in bond distances was calculated from the ESU based on maximum likelihood from PDB entries 5ICU [42] and 5NLT [43], respectively.

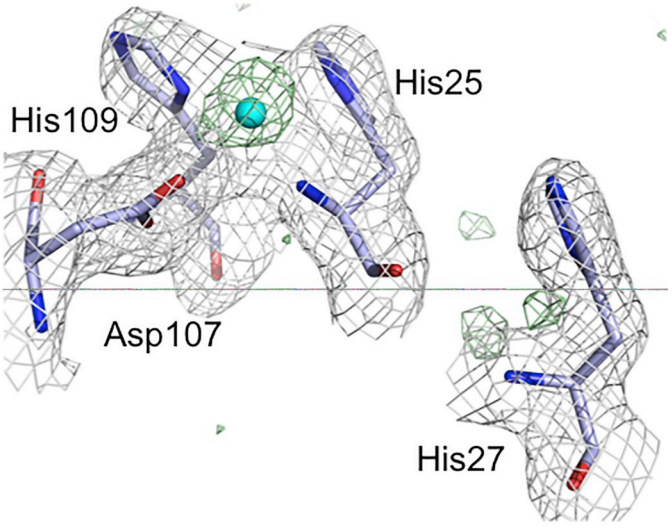

Fig. 3. Coordination environment of the Cu(II) site in $^{Cu(II)WT}$*Pf*-CopC. Electron density map ($2F_o$-F_c map contoured at 1.5σ, colored gray) and difference density map (F_o-F_c map contoured at 3σ with positive density colored green, and copper omitted) of the $^{Cu(II)WT}$*Pf*-CopC Cu(II) site. The Cu(II) atom is shown as a cyan sphere.

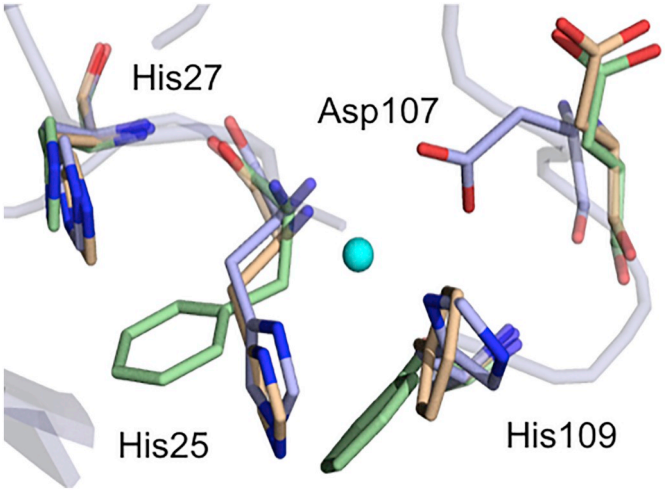

Fig. 4. Conformational changes in the Cu(II) site coordinating ligands and neighboring residues upon mutagenesis of the *Pf*-CopC protein. The structures of the $^{Cu(II)WT}$*Pf*-CopC (light blue), ^{H109F}*Pf*-CopC (wheat) and ^{DM}*Pf*-CopC (pale green) have been superposed. The Cu(II) atom is shown as a cyan sphere.

Table 3
Dissociation constants ($\log K_D$) of CopC family proteins [41].

Protein	Cu(II) binding site	$\log K_D^{abs}$	$\log K_D$ (pH 7.4)
Pf-CopC	NH_2 (H25); 2 N(H25,109); COO^- (D107)	−17.2	−15.6
Ps-CopC	NH_2 (H1); 2 N(H1,91); HOH (W78)	−14.4	−13.7
Ec-PcoC		−14.0	−13.5

spectroscopic and chromatographic analyses and on the binding affinity of *Pf*-CopC for Cu(II) [41]. On this basis, *Pf*-CopC was categorized as a class $C_{0\text{-}2}$ CopC protein and the Cu(II) site was expected to show a different structure to that observed for the class $C_{1\text{-}1}$ (*Ps*-CopC and *Ec*-PcoC) and $C_{0\text{-}1}$ (*Mst*-CopC) proteins. However, the structure presented here shows a Cu(II) binding site (being a 3N + O site) consistent with all structurally characterized proteins from the CopC family to date, and so this protein should be reclassified as a class $C_{0\text{-}1}$ CopC protein [42]. In fact, given this reclassification, we propose that the classes of CopC family proteins can now be reduced to four: $C_{0\text{-}1}$, $C_{1\text{-}1}$, $C_{0\text{-}0}$ and $C_{1\text{-}0}$, with the $C_{0\text{-}1}$ class remaining the most prevalent [42].

3.3. Cu(II)-free structures of the ^{H109F}*Pf*-CopC and ^{DM}*Pf*-CopC proteins

Despite the fact that the mutant proteins ^{H109F}*Pf*-CopC and ^{DM}*Pf*-CopC were submitted to crystallization trials as Cu(II)-loaded proteins, the crystal structures are of the *apo* (copper free) forms. Superposition of the mutant ^{H109F}*Pf*-CopC and ^{DM}*Pf*-CopC protein structures onto that of the $^{Cu(II)WT}$*Pf*-CopC gives r.m.s.d. values of 0.31 Å and 0.39 Å, respectively for 98 common Cα positions, indicating no global structural changes in the presence of the mutations. The absence of Cu(II) and the introduction of Phe residues in place of residues His25 and/or His109 in the ^{H109F}*Pf*-CopC and ^{DM}*Pf*-CopC proteins accompanies a reorientation of the side chains of residues 25 and 109 (Fig. 4). Residues neighboring the H109F mutation, specifically Thr108 and Asp107 also show altered conformations, pointing away from the unoccupied Cu(II) binding sites in the ^{H109F}*Pf*-CopC and ^{DM}*Pf*-CopC structures.

Both the ^{H109F}*Pf*-CopC and ^{DM}*Pf*-CopC mutant proteins were demonstrated to bind Cu(II) at pH 7.4, but with affinities weaker than that of ^{WT}*Pf*-CopC [41], with the ^{DM}*Pf*-CopC protein demonstrated to adopt an ACTUN binding mode with His27 as a Cu(II) ligand [41]. Given the structures described here are Cu-free and the conformation of the side

chain of residue His27 is virtually unchanged between the $^{Cu(II)WT}$*Pf*-CopC and ^{DM}*Pf*-CopC structures, we are unable to propose a mechanism for the generation of the alternative Cu(II) site in ^{DM}*Pf*-CopC. This must await structural determination of the Cu(II)-bound protein.

3.4. Comparison of the structures of the CopC family proteins and their Cu (II)-binding affinities

Superposition of the $^{Cu(II)WT}$*Pf*-CopC structure with those of $^{Cu(II)}$*Mst*-CopC, $^{Cu(II)Cu(I)}$*Ps*-CopC and $^{Cu(II)}$*Tp*-CopC yielded r.m.s.d. values of 1.15 Å, 1.13 Å and 1.43 Å for 70 common Cα positions, respectively. The structural differences between the *Pf*-CopC and *Mst*-CopC proteins predominantly lie in the conformation of β-strand 4, which shows a "dog-leg" [51] arrangement in the *Mst*-CopC structure (Fig. 2). In contrast, the differences between the *Pf*-CopC and *Ps*-CopC structures relate to the conformation of the Cu(I) binding loop in the *Ps*-CopC protein, which is absent in *Pf*-CopC (Fig. 2). It has been suggested that this loop may play a role in protein-protein interactions between Cu(I) binding CopCs and other partner proteins or cognate oxidases [17,34]. The main structural difference between the *Pf*-CopC and *Tp*-CopC proteins is the presence of an additional α-helix in the *Tp*-CopC protein that is not present in the other structurally characterized CopC proteins (Fig. 2). It has been proposed that this α-helix is required for interaction of *Tp*-CopC with partner proteins [43].

The Cu(II) binding affinity of the *Pf*-CopC protein, is significantly different to those of the *Ps*-CopC and *Ec-PcoC* proteins (values for the *Mst*-CopC and *Tp*-CopC proteins are yet to be reported), with $K_{D(Cu(II))}$ for *Pf*-CopC approximately three orders of magnitude lower, indicating significantly tighter binding [41] (Table 3). The Cu(II) binding properties of *Pf*-CopC were suggested to be due to the proposed 4N composition of the Cu(II) binding site [41]. However, the $^{Cu(II)WT}$*Pf*-CopC structure described here shows a Cu(II) binding site composition (a 3N + O site) consistent with all other structurally characterized proteins from the CopC family. What does differ for members of this family is the identity of the residue adjacent to the N-terminal residue (Fig. 1). The *Ps*-CopC and *Ec*-PcoC proteins, with $\log K_{D(Cu(II))} \sim -14$ have Pro residues in this position, compared with *Pf*-CopC ($\log K_{D(Cu(II))} \sim -17$), *Mst*-CopC and *Tp*-CopC with Ala, Ser and Ala residues, respectively. In fact, a recent bioinformatic analysis of sequences from the CopC family of proteins revealed that 171 of 2550 sequences (~7%) show a Pro in this position [42]. We propose that the rigid nature of the Pro side chain in this position in the *Ps*-CopC and *Ec*-PcoC proteins restricts the structural flexibility of the Cu(II) coordination sites and contributes to the observed decreased binding affinities of these proteins for Cu(II). Accordingly, given the presence of residues with increased flexibilities in this position in the *Pf*-CopC, *Mst*-CopC and *Tp*-CopC sequences, we predict the $K_{D(Cu(II))}$ values for *Mst*-CopC and *Tp*-CopC will be similar to that of *Pf*-CopC.

4. Conclusions

The structures presented for the *Pf*-CopC protein are similar to other structurally characterized members of the CopC family of bacterial proteins. In particular, our analyses condense this family to four classes ($C_{0\text{-}1}$, $C_{1\text{-}1}$, $C_{0\text{-}0}$ and $C_{1\text{-}0}$) [42] and classify *Pf*-CopC within the most prevalent class ($C_{0\text{-}1}$). In addition, we propose that the protein sequences, and particularly the identity of the residue adjacent to the N-terminal residue of the mature protein, can serve as predictors of the Cu (II) binding affinities of other family members. The biological consequences of bacteria possessing CopC family proteins that can bind either only Cu(II) or both Cu(I) and Cu(II) with varying binding affinities remains unclear. Whether for example, the propensity of the $C_{0\text{-}1}$ CopC class to bind Cu(II) is linked to the tolerance of various bacteria for copper toxicity will require further investigation.

Acknowledgements

This study was supported by the Australian Research Council grants DP140102746 to MJM and DP130100728 to AGW. Aspects of this research were undertaken on the Macromolecular Crystallography beamline MX2 at the Australian Synchrotron (Victoria, Australia) and we thank the beamline staff for their enthusiastic and professional support.

References

[1] O.M.H. Richter, B. Ludwig, Rev. Physiol. Biochem. Pharmacol. 147 (2003) 47–74.
[2] C. Cervantes, F. Gutierrez-Corona, FEMS Microbiol. Rev. 14 (1994) 121–137.
[3] L. Smith-Mungo, H. Kagan, Matrix Biol. 16 (1998) 387–398.
[4] L. Macomber, J.A. Imlay, Proc. Natl. Acad. Sci. U. S. A. 106 (2009) 8344–8349.
[5] K.Y. Djoko, A.G. McEwan, ACS Chemical Biology, vol. 8, American Chemical Society, 2013, pp. 2217–2223.
[6] C.M. Saporito-Magriñá, R.N. Musacco-Sebio, G. Andrieux, L. Kook, M.T. Orrego, M.V. Tuttolomondo, M.F. Desimone, M. Boerries, C. Borner, M.G. Repetto, Metallomics, vol. 10, The Royal Society of Chemistry, 2018, pp. 1743–1754.
[7] J.M. Arguello, D. Raimunda, T. Padilla-Benavides, Front. Cell. Infect. Microbiol. 3 (2013) 73.
[8] C. Rensing, S.F. McDevitt, Metal Ions in Life Sciences, vol. 12, (2013), pp. 417–450.
[9] K. Bondarczuk, Z. Piotrowska-Seget, Cell Biol. Toxicol. 29 (2013) 397–405.
[10] S. Lutsenko, Curr. Opin. Chem. Biol. 14 (2010) 211–217.
[11] S. Tottey, C. Patterson, L. Banci, I. Bertini, I. Felli, A. Pavelkova, S. Dainty, R. Pernil, K. Waldron, A. Foster, N. Robinson, Proc. Natl. Acad. Sci. U. S. A. 109 (2012) 95–100.
[12] N.J. Robinson, D.R. Winge, Annu. Rev. Biochem. 79 (2010) 537–562.
[13] C. Rensing, G. Grass, FEMS Microbiol. Rev. 27 (2003) 197–213.
[14] M.I. Samanovic, C. Ding, D.J. Thiele, K.H. Darwin, Cell Host Microbe 11 (2012) 106–115.
[15] S.A. Roberts, G.F. Wildner, G. Grass, A. Weichsel, A. Ambrus, C. Rensing, W.R. Montfort, J. Biol. Chem. 278 (2003) 31958–31963.
[16] K.Y. Djoko, L.X. Chong, A.G. Wedd, Z. Xiao, J. Am. Chem. Soc. 132 (2010) 2005–2015.
[17] L. Cortes, A.G. Wedd, Z. Xiao, Metallomics 7 (2015) 776–785.
[18] F. Outten, C. Outten, J. Hale, T. O'Halloran, J. Biol. Chem. 275 (2000) 31024–31029.
[19] F.W. Outten, D.L. Huffman, J.A. Hale, T.V. O'Halloran, J. Biol. Chem. 276 (2001) 30670–30677.
[20] S. Franke, G. Grass, C. Rensing, D.H. Nies, J. Bacteriol. 185 (2003) 3804–3812.
[21] S.A. Gudipaty, M.M. McEvoy, Biochim. Biophys. Acta 1844 (2014) 1656–1661.
[22] F. Long, C.C. Su, M.T. Zimmermann, S.E. Boyken, K.R. Rajashankar, R.L. Jernigan, E.W. Yu, Nature 467 (2010) 484–488.
[23] C.-C. Su, F. Long, M.T. Zimmermann, K.R. Rajashankar, R.L. Jernigan, E.W. Yu, Nature, vol. 470, Nature Publishing Group, a division of Macmillan Publishers Limited, 2011, pp. 558–562. All Rights Reserved.
[24] C.C. Su, F. Long, E.W. Yu, Protein Sci. 20 (2011) 6–18.
[25] E.-H. Kim, D.H. Nies, M.M. McEvoy, C. Rensing, J. Bacteriol. 193 (2011) 2381–2387.
[26] K.N. Chacon, T.D. Mealman, M.M. McEvoy, N.J. Blackburn, Proc. Natl. Acad. Sci. U. S. A. 111 (2014) 15373–15378.
[27] E. Ladomersky, M.J. Petris, Metallomics 7 (2015) 957–964.
[28] S. Chillappagari, M. Miethke, H. Trip, O.P. Kuipers, M.A. Marahiel, J. Bacteriol. 191 (2009) 2362–2370.
[29] D.A. Cooksey, FEMS Microbiol. Rev. 14 (1994) 381–386.
[30] X.X. Zhang, P.B. Rainey, Environ. Microbiol. 10 (2008) 3284–3294.
[31] K. Hirooka, T. Edahiro, K. Kimura, Y. Fujita, J. Bacteriol. 194 (2012) 5675–5687. American Society for Microbiology.
[32] D.A. Rouch, N.L. Brown, Microbiology 143 (1997) 1191–1202 Pt 4.
[33] D.L. Huffman, J. Huyett, F.W. Outten, P.E. Doan, L.A. Finney, B.M. Hoffman, T.V. O'Halloran, Biochemistry 41 (2002) 10046–10055.
[34] K.Y. Djoko, Z. Xiao, A.G. Wedd, ChemBioChem 9 (2008) 1579–1582.
[35] K.Y. Djoko, Z. Xiao, D.L. Huffman, A.G. Wedd, Inorg. Chem. 46 (2007) 4560–4568.
[36] M. Zimmermann, S.R. Udagedara, C.M. Sze, T.M. Ryan, G.J. Howlett, Z. Xiao, A.G. Wedd, J. Inorg. Biochem. 115 (2012) 186–197.
[37] L. Zhang, M. Koay, M.J. Maher, Z. Xiao, A.G. Wedd, J. Am. Chem. Soc. 128 (2006) 5834–5850.
[38] G. Grass, C. Rensing, Biochem. Biophys. Res. Commun. 286 (2001) 902–908.
[39] A.K. Wernimont, D.L. Huffman, L.A. Finney, B. Demeler, T.V. O'Halloran, A.C. Rosenzweig, JBIC, J. Biol. Inorg. Chem. 8 (2003) 185–194.
[40] K. Peariso, D.L. Huffman, J.E. Penner-Hahn, T.V. O'Halloran, J. Am. Chem. Soc. 125 (2003) 342–343.
[41] C.J.K. Wijekoon, T.R. Young, A.G. Wedd, Z. Xiao, Inorg. Chem. 54 (2015) 2950–2959. American Chemical Society.
[42] T.J. Lawton, G.E. Kenney, J.D. Hurley, A.C. Rosenzweig, Biochemistry 55 (2016) 2278–2290.
[43] E.M. Osipov, A.V. Lilina, S.I. Tsallagov, T.N. Safonova, D.Y. Sorokin, T.V. Tikhonova, V.O. Popov, Acta Crystallogr. D 74 (2018) 632–642.
[44] C. Harford, B. Sarkar, Acc. Chem. Res. 30 (1997) 123–130. American Chemical Society.

[45] Z. Otwinowski, W. Minor, Methods Enzymol, vol. 276, Academic Press, 1997, pp. 307–326.
[46] A.J. McCoy, R.W. Grosse-Kunstleve, P.D. Adams, M.D. Winn, L.C. Storoni, R.J. Read, J. Appl. Crystallogr. 40 (2007) 658–674.
[47] M.D. Winn, C.C. Ballard, K.D. Cowtan, E.J. Dodson, P. Emsley, P.R. Evans, R.M. Keegan, E.B. Krissinel, A.G. Leslie, A. McCoy, S.J. McNicholas, G.N. Murshudov, N.S. Pannu, E.A. Potterton, H.R. Powell, R.J. Read, A. Vagin, K.S. Wilson, Acta Crystallogr. D Biol. Crystallogr. 67 (2011) 235–242.
[48] N. Stein, J. Appl. Crystallogr. 41 (2008) 641–643.
[49] G.N. Murshudov, P. Skubak, A.A. Lebedev, N.S. Pannu, R.A. Steiner, R.A. Nicholls, M.D. Winn, F. Long, A.A. Vagin, Acta Crystallogr. D Biol. Crystallogr. 67 (2011) 355–367.
[50] V.B. Chen, W.B. Arendall 3rd, J.J. Headd, D.A. Keedy, R.M. Immormino, G.J. Kapral, L.W. Murray, J.S. Richardson, D.C. Richardson, Acta Crystallogr. D Biol. Crystallogr. 66 (2010) 12–21.
[51] M.E. Murphy, P.F. Lindley, E.T. Adman, Protein Sci. 6 (1997) 761–770.